APPLIED SCIENCES AND ENGINEERING

Sequential self-folding of polymer sheets

Ying Liu, Brandi Shaw, Michael D. Dickey,* Jan Genzer*

Shape plays an important role in defining the function of materials, particularly those found in nature. Several strategies exist to program materials to change from one shape to another; however, few can temporally and spatially control the shape. Programming the sequence of shape transformation with temporal control has been driven by the desire to generate complex shapes with high yield and to create multiple shapes from the same starting material. This paper demonstrates a markedly simple strategy for programmed self-folding of two-dimensional (2D) polymer sheets into 3D objects in a sequential manner using external light. Printed ink on the surface of the polymer sheets discriminately absorbs light on the basis of the wavelength of the light and the color of the ink that defines the hinge about which the sheet folds. The absorbed light gradually heats the underlying polymer across the thickness of the sheet, which causes relief of strain to induce folding. These color patterns can be designed to absorb only specific wavelengths of light (or to absorb differently at the same wavelength using color hues), thereby providing control of sheet folding with respect to time and space. This type of shape programming may have numerous applications, including reconfigurable electronics, actuators, sensors, implantable devices, smart packaging, and deployable structures.

INTRODUCTION

Nature abounds with structures that change their shapes in response to external stimuli. Examples of these responses include the unfolding of conifer pinecones during drying, rapid snapping of the Venus flytrap in response to touch, differential growth of plants toward sunlight (that is, phototropism and heliotropism), or blossoming of flowers in response to temperature or light (*1*–*13*). A great challenge for scientists and engineers is to mimic the behavior that nature has perfected over billions of years in man-made, nonliving materials. These types of man-made shape-programmable materials are attractive for many applications, including reconfigurable devices (*14*–*17*), sensors and actuators (*18*–*22*), deployable objects (*23*, *24*), robotics (*16*, *25*, *26*), actuators and walkers (*15*, *20*, *27*–*29*), and implantable devices (*30*).

There are many materials that can be programed to change shape on command (*31*–*39*). Examples of these materials include shape memory polymers and alloys that change shape in response to heat, hydrogels that swell in response to moisture, and bimorphs that bend because of differences in thermal expansion or because of expansion caused by solvent swelling. With a few exceptions, these strategies transform materials from an initial shape to a single final shape and include "four-dimensional (4D) printing," which converts a 3D-printed part from one shape to another by incorporating responsive materials (*40*–*42*). In addition, the shape change usually occurs simultaneously throughout the material. Programming materials to change shape in a defined spatial and temporal sequence enables the formation of multiple 3D forms from the same initial starting material, which is appealing because shape plays an important role in defining the function of materials. Sequential events are important in biological systems (protein or DNA folding) (*43*), macroscopic assembly (packaging, construction, and storage), locomotion (*44*), unfolding of leaves (*45*), and differential growth of plants (*6*).

Despite its importance, only a few solutions exist for sequential shape transformation of man-made materials. One approach involves focusing an external stimulus to local regions on the material. An example of this approach is directing thermal energy to local regions on a responsive surface by focused light (*46*) or by patterned Joule heaters (*14*, *47*). Other approaches involve patterning two or more materials to respond to the same stimulus with different degrees (*41*, *48*) or respond independently to multiple distinct stimuli. These methods require multistep fabrication or complex (and sometimes, incompatible) sequences of stimuli.

We sought a strategy to control the sequential formation of shapes with respect to time and space. Folding, inspired by the ancient art of origami, offers one route to alter the shape of a sheet of material. Although origami involves folding paper by hand, the concept of folding can be extended to materials beyond paper, and the folding itself can be programmed by material design and be executed in a hands-free manner.

Self-folding is a deterministic assembly process that enables predesigned planar templates, which are compatible with planar processing (for example, lithography and printing), to transform into 3D structures (*49*, *50*). Self-folding of polymeric materials is particularly compelling because of the potential of using materials that are biocompatible, flexible, durable, low-cost, and lightweight. Self-folding of sheets can be accomplished using several methodologies. Most of these approaches are based on synchronous folding, that is, folding of all hinges at the same time (*31*, *32*, *34*, *37*, *38*, *49*, *51*).

Recently, we introduced a simple method for self-folding of prestrained polymer sheets (*52*). The process uses a desktop printer to pattern black ink onto the sheets, followed by irradiation with light. The inked regions on the specimen preferentially absorb the light and convert it into heat, which, in turn, causes a localized gradient of shrinkage across the thickness of the polymer sheet. This shrinkage induces the sheet to fold within seconds. Here, we achieve sequential folding in an equally simple manner by laserjet-printing colored ink to define "hinges." In this case, a "hinge" is simply a region of the sheet that has ink printed on it. When irradiated with a narrow wavelength of light [originating from light-emitting diodes (LEDs)], only the hinges printed with colors that absorb that wavelength heat up, causing selective folding by localized shrinkage. This strategy offers a markedly simple method for remotely controlling the time scale, direction, and sequence of folding using parameters that can be controlled readily by a printer and the wavelength of the external source of light.

Sequential self-folding (called "sequential folding" in this paper), defined simply as folding with temporal and spatial control of multiple

Department of Chemical and Biomolecular Engineering, North Carolina State University, 911 Partners Way, Raleigh, NC 27695, USA.
*Corresponding author. Email: mddickey@ncsu.edu (M.D.D.); jgenzer@ncsu.edu (J.G.)

hinges printed onto the same polystyrene (PS) sheet, can thus be achieved by using selective absorption of light. This strategy enables sequential shape programming in a simple and controllable hands-free manner.

RESULTS AND DISCUSSION

Differential optical absorption

Our approach to self-folding relies on differential light absorption. The pristine prestrained polymer sheets are optically transparent in the visible range and can therefore be exposed indefinitely to light in the visible regime without any response. The use of colored hinges that selectively absorb (or transmit) light of a given wavelength enables sequential folding. The radar plot (Fig. 1A) highlights the absorption of blue, green, and red light by different colors of ink printed on a plain, transparent polymer sheet. For example, the yellow and cyan inks show an opposite absorption response to red and blue LEDs. In contrast to black or grayscale inks, which absorb light indiscriminant of wavelength (*52*, *53*), the folding sequence of a sheet containing yellow and cyan hinges depends entirely on the order of exposure to light, as shown in Fig. 1B. The cyan hinge only folds in response to 660-nm light, whereas it remains unresponsive to 470-nm light even after extended exposures (at least 10 min), as shown in Fig. 1C. Concurrently, the yellow hinge only folds in response to 470-nm light, whereas it remains unresponsive to 660-nm light for at least 10 min. This simple idea can be extended to other color pairs with different LED wavelengths (Fig. 1D). The UV-vis absorption spectra of different color inks at wavelengths ranging from 300 to 800 nm are provided in fig. S1. More details about the LEDs and inks are provided in tables S1 and S2.

Sequential folding using colored hinges to achieve complex structures

This approach can sequentially fold complex 3D structures, in which the order of the folding affects the final shape. We designed, printed, and tested different colored hinge patterns for fabricating 3D structures

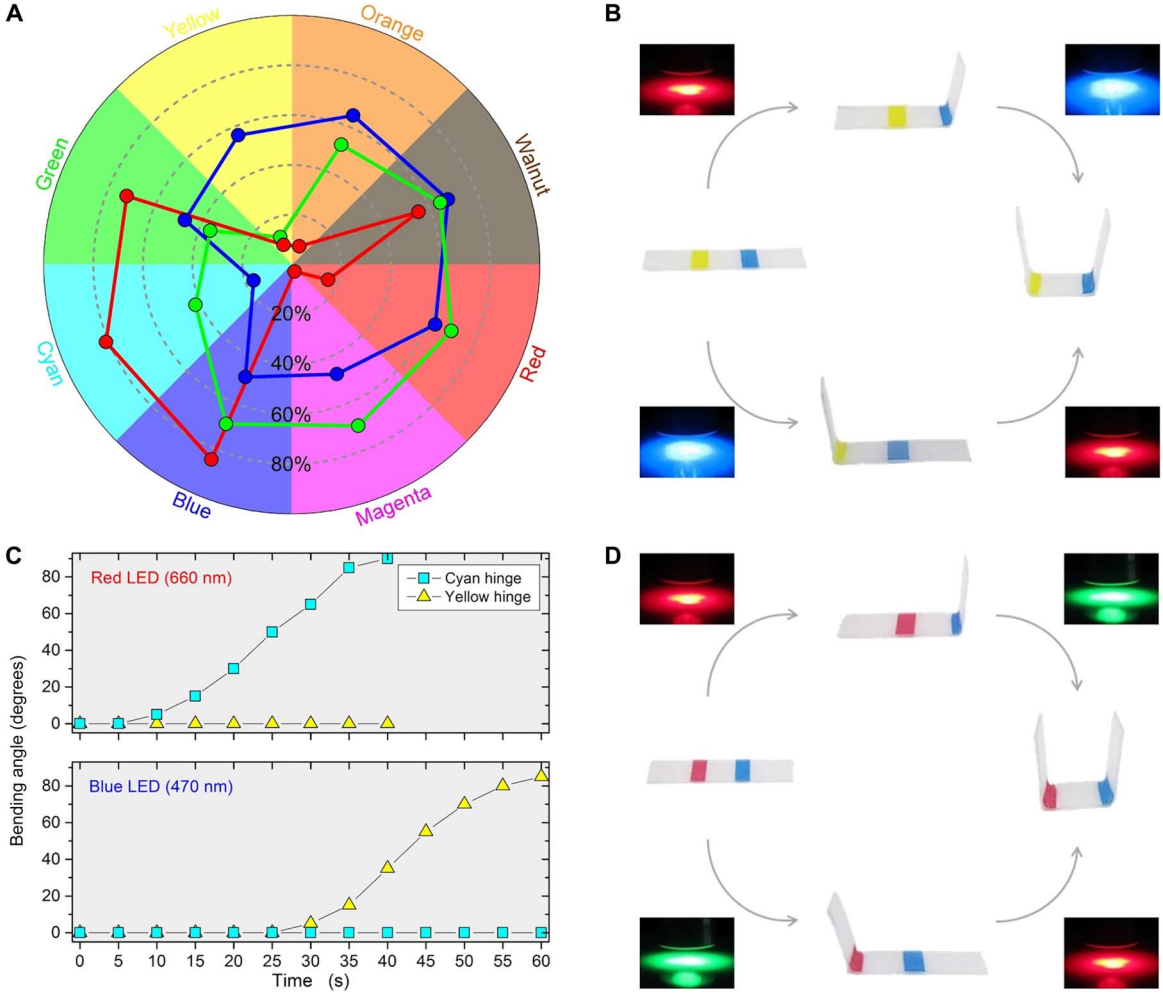

Fig. 1. Concept of differential light absorption for sequential folding. (**A**) Radar plot in which each wedge represents an ink color from a laserjet printer. Data points represent the optical absorption of the three wavelengths of LEDs used in this study: red (660 nm), green (530 nm), and blue (470 nm) LEDs. The data points are connected by lines to guide the eye. (**B**) Photographs for folding controlled in sequence by using hinges in yellow (in response to a blue LED) and cyan (in response to a red LED). Fifteen-watt LEDs were used at ~1.5 cm above the sample. (**C**) Bending angle as a function of LED exposure time for yellow and cyan hinges under the exposure of red and blue LEDs. (**D**) Photographs for folding controlled in sequence by using the hinges in magenta (in response to a green LED) and cyan (in response to a red LED). Fifteen-watt red LED was used at ~1.5 cm away from the sample, and 15-W green LED was used at a distance of 0.7 cm. The sample dimensions are 18 mm × 5 mm with a hinge width of 2 mm.

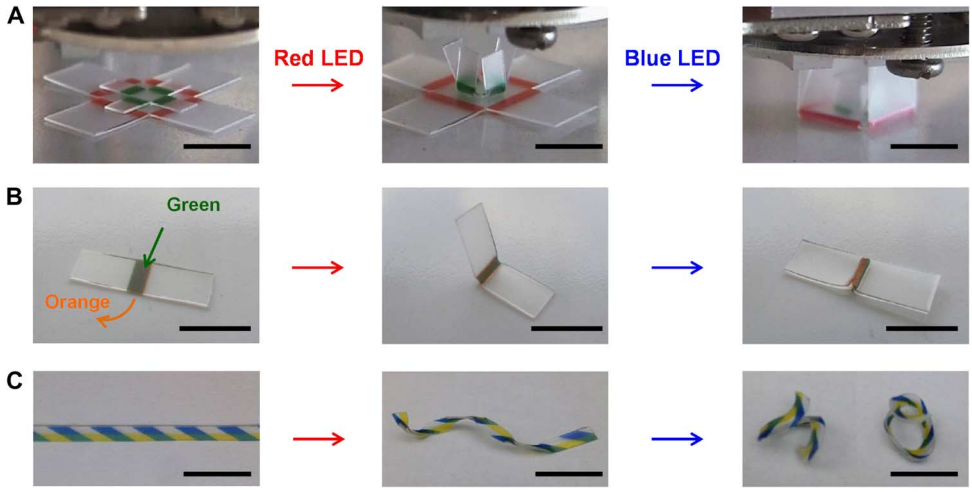

Fig. 2. Images of complex structures formed via sequential folding. (**A**) Nested boxes with a small box with green hinges (5 mm × 5 mm × 5 mm) on top of a large one with orange hinges (10 mm × 10 mm × 10 mm). (**B**) Unfolding pathway: Folding first occurs toward the top green hinge using a red LED. An orange hinge is patterned on the opposite side of the green hinge. Unfolding occurs by activating the orange hinge using a blue LED. (**C**) Supercoil formed in a polymer strip patterned with yellow (width, 1.5 mm) and cyan (width, 2.0 mm) diagonal stripes. Scale bars, 10 mm.

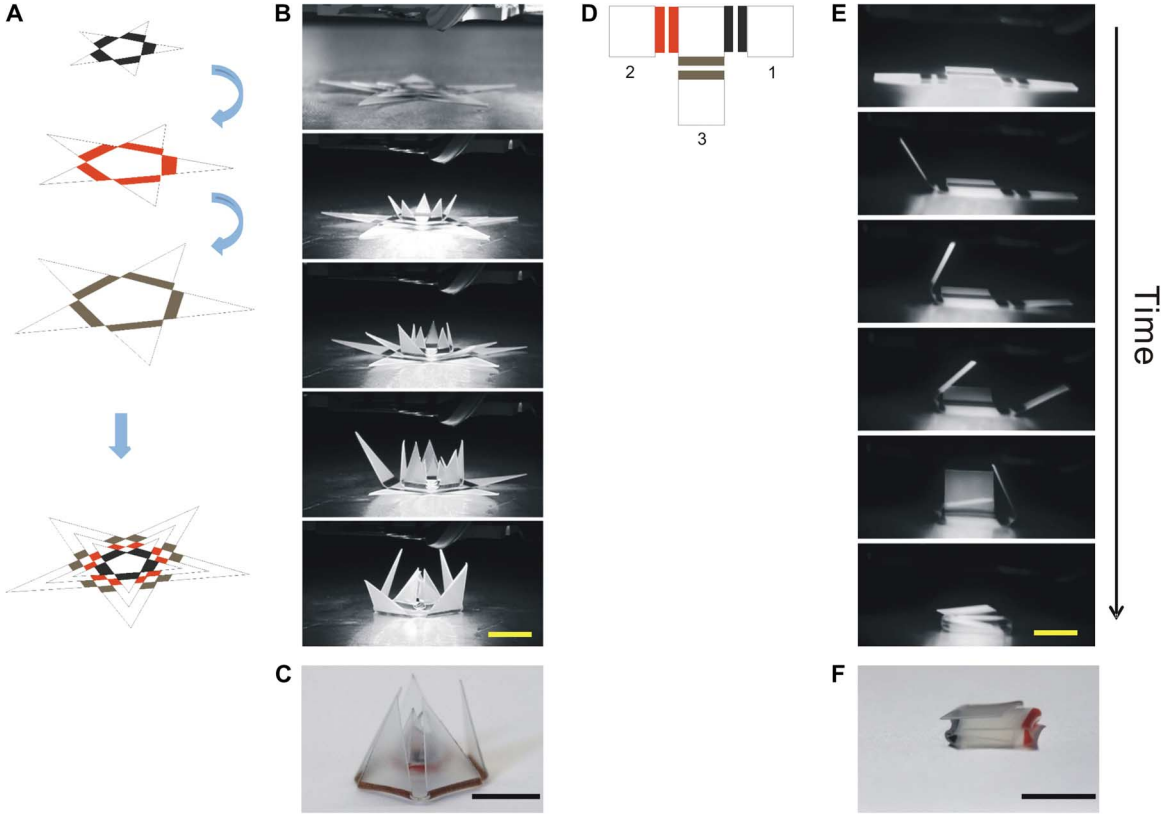

Fig. 3. Complex geometries via sequential folding. (**A**) Perspective schematic of star-shaped templates featuring a small star (black hinges) placed on the top of a medium-sized star (red hinges) placed on top of the largest star (walnut-colored hinges). All hinge widths are 2 mm. (**B**) Corresponding sequential folding of the three-layer lotus made of three stars with five hinges placed on top of each other. Onset time for these snapshots are 0 s (top) and 3, 4, 6, and 16 s (bottom) (see video S1 in the Supplementary Materials). (**C**) Photograph of a folded structure. (**D**) Schematic of a template featuring double hinges with black, red, and walnut colors patterned on a polymer sheet. Numbers 1 to 3 denote the designed folding order of the three panels. The double-line hinges are 2.0 mm wide with a spacing of 1.0 mm between the two lines. (**E**) Three independent but overlapping single folding panels self-fold sequentially. The double-hinge design facilitates folding up to 180°. Time for these snapshots are 1 s (top) and 2, 3, 5, 7, and 25 s (bottom) (see video S2 in the Supplementary Materials). (**F**) Photograph of a folded structure. Scale bars, 10 mm.

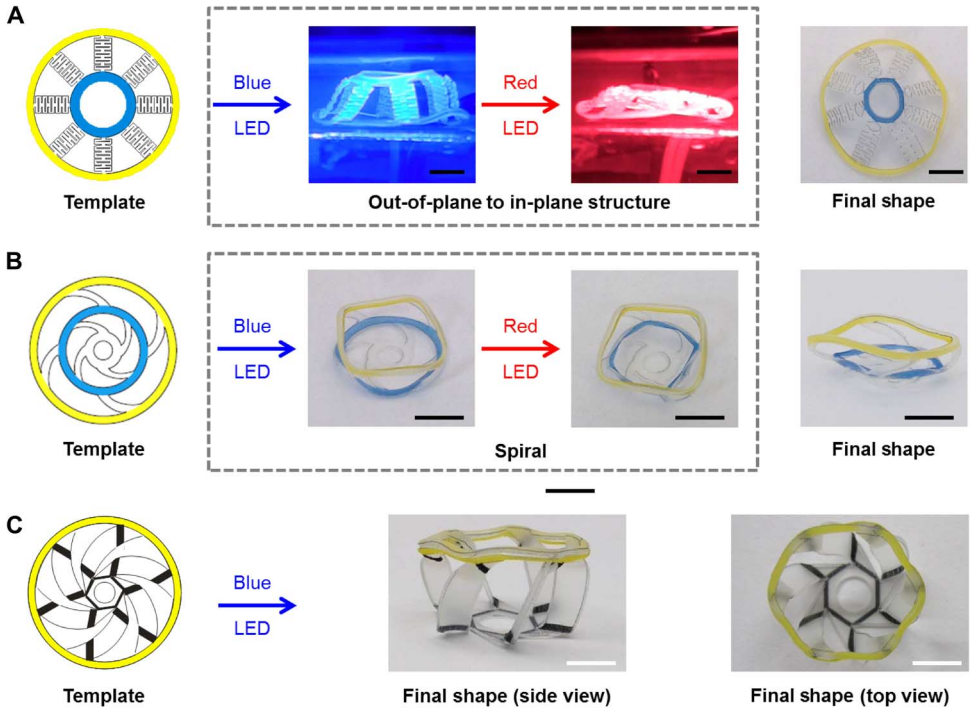

Fig. 4. Sequentially actuated kirigami 3D shapes. (**A**) Out-of-plane and in-plane structures are actuated sequentially by shrinking the outer ring (yellow) first to achieve out-of-plane motion and then shrinking the inner ring (cyan) to flatten the sample again. Living hinges connect the two circular rings. (**B**) The spiral structure forms by first pushing upward the bottom because of the shrinkage of the yellow ring and subsequently pushing upward the middle layer because of the shrinkage of the cyan ring. Images in the boxes with dashed lines show the temporary shape formed by irradiating with blue LED and then the shape formed by irradiating with a red LED sequentially. The final shape represents a side view of the spiral. (**C**) A dome structure results by applying inks with different optical absorption under a blue LED. The samples are held at 90°C in a custom-built convection oven during folding. Scale bars, 5 mm.

by sequential folding. Figure 2 depicts the sequential folding of colored hinges triggered in sequence by exposure to a red LED and then a blue LED. Figure 2A shows the sequential folding of nested boxes, inspired by a "Matryoshka doll." A smaller box with green hinges folds during exposure to a red LED, whereas the larger box featuring orange hinges remains flat, which is consistent with absorption measurements in fig. S1. The larger box with orange hinges folds after switching to a blue LED.

Another application of sequential folding is the ability to fold and then unfold. Figure 2B demonstrates that exposure to a red LED causes the green hinge (printed on the top of the prestrained polymer sheet) to fold. Exposure of the folded sample to a blue LED causes the orange hinge printed on the opposite side of the polymer sheet to fold in the opposite direction, rendering the sample flat. In addition, Fig. 2C shows that more complex structures, such as linear supercoils, are possible. The coil first forms during folding of the cyan diagonal stripes using a red LED. Subsequent exposure to a blue LED shrinks the yellow hinges to produce the supercoil. This supercoiling, to a first approximation, is analogous to the supercoiling of DNA molecules (twisting of a DNA double helix around its own axis in 3D structures), although DNA supercoiling is a much more complicated phenomenon (*54*).

The absorbance of a given color varies with the wavelength of light in a nonmonotonic manner (compare fig. S1). Although the examples in Figs. 1 and 2 take advantage of inks that absorb at the extremes of this scale, it is possible to harness intermediate values of absorbance to control the time scales of sequential folding in response to a single light source. Conceptually, the use of different hues (that is, colors that have intermediate values of light absorption at the same wavelength) is similar to using grayscales to control the time scales of folding (*53*, *55*).

Figure 3 depicts examples of the sequential folding using different color hinges triggered by a single LED. In this example, a "lotus flower," composed of three vertically stacked sheets with the same star-like shapes of different sizes and different colored hinges, closes sequentially (Fig. 3, A to C). A small star with a black hinge folds first because the black ink has the highest degree of light absorption. The stars at the middle (red hinge) and bottom (walnut-colored hinge) then fold in sequence due to differential light absorption (video S1 depicts real-time folding).

Figure 3 (D to F) shows a folded structure with three independent but overlapping single folding panels. In the absence of sequential control, these panels would collide during folding. However, this multilayer structure is possible by controlling the sheet folding sequence. The panel with black hinges folds first, as noted in Fig. 3D, because it has the highest absorption of light, followed by the panel with red hinges. The panel with walnut-colored hinges folds last. A paper-folding mimetic with overlapped layers is possible using this method (S2 depicts real-time folding).

The art of "kirigami" (that is, paper art by cutting) can be applied to polymer sheets to increase the local flexibility and to facilitate otherwise prohibited modes of motion (*56*–*58*). The concept of a "living hinge" has been used for flexible connections in packaging and microelectromechanical systems (*59*–*61*). Figure 4 depicts the application of kirigami in sequential folding to realize significant out-of-plane motion from in-plane shrinkage. For instance, a cylindrical "gripper" can be realized using a planar template of two circular rings

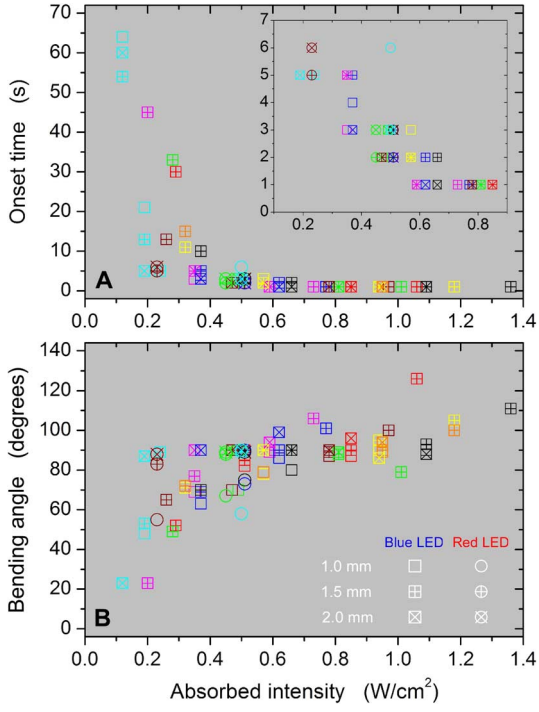

Fig. 5. Generalized onset time and bending angle. Effect of light intensity absorbed by the hinge on (**A**) the onset of folding and (**B**) of bending angle for blue (squares) and red (circles) LEDs. The symbol colors correspond to the color of the inks printed as hinges, as described in table S2 (color code). Onset times and bending angles refer to hinges printed on Grafix polymer sheets using the setup detailed in Materials and Methods. Inset depicts the zoom-in plot for the data with onset time of 0 to 8 s. The sample dimensions are 25 mm × 10 mm with a central hinge width of 2 mm.

connected with living hinges, as shown in Fig. 4A. The outer circular ring (in yellow) shrinks to generate a "closed" position using a blue LED, which is possible because of the connections of the flexible living hinges. The inner circular ring (in cyan) shrinks separately to flatten the gripper upon subsequent exposure to a red LED. Similarly, a spiral structure can be achieved, as shown in Fig. 4B. The final shape looks like a tower in which each layer can pop up one by one if each circular ring is printed in a different color. In addition, a kirigami dome structure (Fig. 4C) can be generated using a blue LED, in which the panels with black hinges fold slightly ahead of the shrinkage of the outer ring (in yellow) to promote break symmetry and thereby the formation of the raised dome shape.

Impact of energy absorption on sequential folding

This strategy for sequential folding relies on selectively delivering energy from an external light source to heat hinges with different colors printed on polymer sheets. The intensity and wavelength of light and its absorption by the printed ink (determined by the color of the ink) are the three key parameters in this strategy for sequential self-folding. High light intensity combined with high absorption of ink color induces the most rapid folding. The delivery of energy density (W/cm^2) can be characterized by multiplying the intensity of light (W/cm^2) and its percent absorption by the ink (%). Figure 5 summarizes the combined effect of the absorbed intensity of light on the onset time of folding. The onset time is defined as the amount of time that the sample is exposed to external light before it starts to fold. These data contain a wide range of samples patterned with hinges of different colors and exposed using two different LEDs. The data in Fig. 5 fall on master curves, indicating a universal behavior for onset time and bending angle for all hinge widths, hinge ink colors, and wavelength of light studied in this work.

The onset time decreases monotonically with increasing absorbed energy (Fig. 5A); the decrease is initially rapid for an absorbed energy of <0.5 W/cm^2. The onset time remains very short for higher values of absorbed energy, where folding occurs rapidly. Concurrently, the bending angle increases with increasing absorbed energy and reaches a value of ~90° at high absorbed energies (compare Fig. 5B). The change in bending angle with respect to absorbed energy increases rapidly for an absorbed energy of <0.5 W/cm^2 and more gradually for higher values of absorbed energy. The trends depicted in Fig. 5 thus serve as guides in designing systems for sequential folding, where one needs to discriminate among multiple folding pathways by judiciously choosing the right combination of hinge width, hinge color, and wavelength of light to achieve the desired folding angle and onset time for folding.

Our previous study of folding black hinges determined that the onset time and folding angle depend, in a complex way, on the flux of light and the hinge geometry because of the dynamic impact of heat dissipation across the polymer sheet and into the environment (*62*). From this previous work, for hinge widths ranging from 1.0 to 2.0 mm and a hinge length of 10 mm (identical to those in this work), the calculated power density threshold needed to achieve folding is in the range of 0.3 to 0.6 W/cm^2. The data in Fig. 5 for color hinges agree with these previous findings. The scatter in onset time and bending angle (at absorbed energies of <0.5 W/cm^2 and a bending angle at high absorbed energies) is likely due to significant heat dissipation to the polymer outside the inked regions.

CONCLUSIONS

This paper demonstrates a simple approach to realize and control sequential folding of 3D shapes. The method uses a desktop printer to pattern inks of different light absorptivity as hinges on otherwise homogeneous prestrained polymer (for example, PS) sheets. Hinges of different colors printed onto the same sheet fold sequentially depending on the wavelength of light by which they are irradiated. This method only requires one-step printing on a 2D polymer substrate and flood exposure of light to create complex 3D shapes in a controllable, predictable, and sequential manner. The appeal of this technique is that it uses a single type of uniform stimuli (light) to sequentially fold a homogeneous material (polymer sheet) patterned by printing. The demonstrations here use thin (~0.3 mm) sheets of PS, but the concept of localized heating should extend to other shape memory polymers, including those that are nonplanar or thicker (*63*). Currently, the method is capable of folding and unfolding hinges once, but the development of reversible shape memory polymers should enable even more complex and repeatable deformations (*64*–*69*).

Although we used commercial inks, this method can be further extended, in principle, by applying alternative absorbers, such as nanoparticles that exhibit distinct light absorption at specified wavelengths, including those outside the visible regime. Other 2D printing strategies should also work equally well. Printing these active materials on prestrained polymers may further extend the applicability of the present method to form 3D objects from 2D patterns or even 3D objects that change shape in response to light.

MATERIALS AND METHODS

Clear inkjet shrink film (Grafix) with a film thickness of 0.3 mm was used as the prestrained polymer sheet. These prestrained polymer sheets shrunk in-plane up to ~55% of its original size while heating over the transition temperature (~105°C) (*52*). An HP Color LaserJet CP3525dn printer produced 2D color ink patterns, which were designed in CorelDRAW. The templates were cut with scissors, and the kirigami templates were cut with a laser cutter. The thickness of the printed hinges on the substrate using this printer was ~5.4 ± 1.3 μm for all colors (assessed by profilometry, Veeco Dektak) (see fig. S2 for details). Fifteen-watt red (660 nm), blue (470 nm), and green (530 nm) LEDs (purchased from LEDSupply) and 50-W red (630 nm) and blue (470 nm) LEDs (purchased from LED Hero) were used as the heating sources. Fifteen-watt handheld LEDs were used for the conceptual demonstration of sequential self-folding in Fig. 1. Fifty-watt LEDs with a large irradiation area (40 mm × 40 mm) were used to investigate the impact of the key parameters and to offer more uniform light exposure for the folding demonstrations in Figs. 2 to 4. The absorptions of ink of different colors at 630 nm (wavelength for 50-W LED) and 660 nm (wavelength for 15-W LED) are almost the same as shown in fig. S1. Dimensions of samples studied for the conceptual demonstration and various folding structures have been described in Figs. 1 to 5. In our self-folding tests, the samples were carried on a hot plate (EchoTherm HS30, Torrey Pines Scientific) at the preheating temperature of 90°C, which is below but close to the transition temperature of shrinking, to facilitate fast folding. In some cases, we replaced the hot plate with a custom-built convection heating chamber (that is, data in Fig. 4) to assure uniform preheating temperature to the whole sample during folding. A 50-W red LED was placed 1.5 cm away from the surface of the sample, and a 50-W blue LED was placed 2 cm away from the surface of the sample to obtain reasonable high energy intensity and leave sufficient space between the LED and the hot plate to allow for the folding motion. The bending angles of all samples were recorded by a video camera (Canon VIXIA HF S20). The bending angles were measured by a protractor.

SUPPLEMENTARY MATERIALS

Supplementary material for this article is available at http://advances.sciencemag.org/cgi/content/full/3/3/e1602417/DC1

fig. S1. Optical absorption spectra of color inks printed on a plain prestrained polymer sheet.
fig. S2. Thickness of hinges printed with different colors using an HP Color LaserJet CP3525dn printer on Grafix polymer sheets.
table S1. Measured power density for different LEDs used for the folding test.
table S2. CMYK codes for different colors.
video S1. Sequential self-folding of three star-shaped templates placed on top of each other using a blue LED.
video S2. Sequential self-folding of a template featuring double hinges with different colors on the three panels to fold up to 180°.

REFERENCES AND NOTES

1. M. Taya, R. Stahlberg, F. Li, Y. J. Zhao, Sensors and actuators inherent in biological species. *Proc. SPIE.* **6529**, 652902 (2007).
2. A. R. Studart, Biologically inspired dynamic material systems. *Angew. Chem. Int. Ed.* **54**, 3400–3416 (2015).
3. B. J. Atwell, P. E. Kriedemann, C. G. N. Turnbull, *Plants in Action: Adaptation in Nature, Performance in Cultivation* (Macmillan Education Australia, 1999).
4. C. Darwin, *The Power of Movement in Plants* (D. Appleton & Company, 1881).
5. N. M. Wereley, J. M. Sater, *Plants and Mechanical Motion: A Synthetic Approach to Nastic Materials and Structures* (DEStech Publications, 2012).
6. H. Liang, L. Mahadevan, Growth, geometry, and mechanics of a blooming lily. *Proc. Natl. Acad. Sci. U.S.A.* **108**, 5516–5521 (2011).
7. M. P. M. Dicker, J. M. Rossiter, I. P. Bond, P. M. Weaver, Biomimetic photo-actuation: Sensing, control and actuation in sun-tracking plants. *Bioinspir. Biomim.* **9**, 36015 (2014).
8. L. Yao, J. Ou, C.Y. Cheng, H. Steiner, W. Wang, G. Wang, H. Ishii, bioLogic: Natto cells as nanoactuators for shape changing interfaces, in *Proceedings of the 33rd Annual ACM Conference on Human Factors in Computing Systems* (ACM, 2015), pp. 1–10.
9. Y. Forterre, J. M. Skotheim, J. Dumais, L. Mahadevan, How the Venus flytrap snaps. *Nature* **433**, 421–425 (2005).
10. S. E. Williams, A. B. Bennett, Leaf closure in the Venus Flytrap: An acid growth response. *Science* **218**, 1120–1122 (1982).
11. H. Kobayashi, B. Kresling, J. F. V. Vincent, The geometry of unfolding tree leaves. *Proc. R. Soc. Lond. B* **265**, 147–154 (1998).
12. W. G. van Doorn, U. Van Meeteren, Flower opening and closure: A review. *J. Exp. Bot.* **54**, 1801–1812 (2003).
13. A. K. Stowers, D. Lentink, Folding in and out: Passive morphing in flapping wings. *Bioinspir. Biomim.* **10**, 25001 (2015).
14. E. Hawkes, B. An, N. M. Benbernou, H. Tanaka, S. Kim, E. D. Demaine, D. Rus, R. J. Wood, Programmable matter by folding. *Proc. Natl. Acad. Sci. U.S.A.* **107**, 12441–12445 (2010).
15. F. Ilievski, A. D. Mazzeo, R. F. Shepherd, X. Chen, G. M. Whitesides, Soft robotics for chemists. *Angew. Chem. Int. Ed.* **50**, 1890–1895 (2011).
16. S. Felton, M. Tolley, E. Demaine, D. Rus, R. Wood, A method for building self-folding machines. *Science* **345**, 644–646 (2014).
17. M. Zarek, M. Layani, I. Cooperstein, E. Sachyani, D. Cohn, S. Magdassi, 3D printing of shape memory polymers for flexible electronic devices. *Adv. Mater.* **28**, 4146 (2016).
18. J.-H. Cho, M. D. Keung, N. Verellen, L. Lagae, V. V. Moshchalkov, P. V. Dorpe, D. H. Gracias, Nanoscale origami for 3D optics. *Small* **7**, 1943–1948 (2011).
19. W. Jiang, D. Niu, H. Liu, C. Wang, T. Zhao, L. Yin, Y. Shi, B. Chen, Y. Ding, B. Lu, Photoresponsive soft-robotic platform: Biomimetic fabrication and remote actuation. *Adv. Funct. Mater.* **24**, 7598–7604 (2014).
20. T. G. Leong, C. L. Randall, B. R. Benson, N. Bassik, G. M. Stern, D. H. Gracias, Tetherless thermobiochemically actuated microgrippers. *Proc. Natl. Acad. Sci. U.S.A.* **106**, 703–708 (2009).
21. L. Ionov, Biomimetic hydrogel-based actuating systems. *Adv. Funct. Mater.* **23**, 4555–4570 (2013).
22. E. Brown, N. Rodenberg, J. Amend, A. Mozeika, E. Steltz, M. R. Zakin, H. Lipson, H. M. Jaeger, Universal robotic gripper based on the jamming of granular material. *Proc. Natl. Acad. Sci. U.S.A.* **107**, 18809–18814 (2010).
23. C. J. Pentlicki, U.S. Patent 4,133,501A (1979).
24. S. A. Zirbel, R. J. Lang, M. W. Thomson, D. A. Sigel, P. E. Walkemeyer, B. P. Trease, S. P. Magleby, L. L. Howell, Accommodating thickness in origami-based deployable arrays. *J. Mech. Des.* **135**, 111005 (2013).
25. S. M. Felton, M. T. Tolley, C. D. Onal, D. Rus, R. J. Wood, Robot self-assembly by folding: A printed inchworm robot, in *2013 IEEE International Conference on Robotics and Automation (ICRA)* (IEEE, 2013), pp. 277–282.
26. M. T. Tolley, R. F. Shepherd, M. Karpelson, N. W. Bartlett, K. C. Galloway, M. Wehner, R. Nunes, G. M. Whitesides, R. J. Wood, An untethered jumping soft robot, in *2014 IEEE/RSJ International Conference on Intelligent Robots and Systems (IROS)* (IEEE/RSJ, 2014), pp. 561–566.
27. L. Ionov, Hydrogel-based actuators: Possibilities and limitations. *Mater. Today* **17**, 494–503 (2014).
28. J. Ryu, M. D'Amato, X. Cui, K. N. Long, H. J. Qi, M. L. Dunn, Photo-origami–Bending and folding polymers with light. *Appl. Phys. Lett.* **100**, 161908 (2012).
29. A. T. Sellinger, D. H. Wang, L.-S. Tan, R. A. Vaia, Electrothermal polymer nanocomposite actuators. *Adv. Mater.* **22**, 3430–3435 (2010).
30. C. M. Yakacki, R. Shandas, C. Lanning, B. Rech, A. Eckstein, K. Gall, Unconstrained recovery characterization of shape-memory polymer networks for cardiovascular applications. *Biomaterials* **28**, 2255–2263 (2007).
31. Y. Liu, J. Genzer, M. D. Dickey, 2D or not 2D: Shape programming of polymer sheets. *Prog. Polym. Sci.* **52**, 79–106 (2015).
32. E. A. Peraza-Hernandez, D. J. Hartl, R. J. Malak Jr., D. C. Lagoudas, Origami-inspired active structures: A synthesis and review. *Smart Mater. Struct.* **23**, 94001 (2014).
33. R. Kempaiah, Z. Nie, From nature to synthetic systems: Shape transformation in soft materials. *J. Mater. Chem. B* **2**, 2357–2368 (2014).
34. D. H. Gracias, Stimuli responsive self-folding using thin polymer films. *Curr. Opin. Chem. Eng.* **2**, 112–119 (2013).
35. R. Vaia, J. Baur, Adaptive composites. *Science* **319**, 420–421 (2008).
36. R. Geryak, V. V. Tsukruk, Reconfigurable and actuating structures from soft materials. *Soft Matter.* **10**, 1246–1263 (2014).
37. L. Ionov, Soft microorigami: Self-folding polymer films. *Soft Matter.* **7**, 6786–6791 (2011).
38. D. Chen, J. Yoon, D. Chandra, A. J. Crosby, R. C. Hayward, Stimuli-responsive buckling mechanics of polymer films. *J. Polym. Sci. B Polym. Phys.* **52**, 1441–1461 (2014).
39. L. Ionov, Polymeric actuators. *Langmuir* **31**, 5015–5024 (2015).
40. S. Tibbits, 4D printing: Multi-material shape change. *Archit. Design* **84**, 116–121 (2014).

41. Y. Mao, K. Yu, M. S. Isakov, J. Wu, M. L. Dunn, H. J. Qi, Sequential self-folding structures by 3D printed digital shape memory polymers. *Sci. Rep.* **5**, 13616 (2015).
42. A. S. Gladman, E. A. Matsumoto, R. G. Nuzzo, L. Mahadevan, J. A. Lewis, Biomimetic 4D printing. *Nat. Mater.* **15**, 413–418 (2016).
43. R. Honda, J.-i. Wakita, M. Katori, Self-elongation with sequential folding of a filament of bacterial cells. *J. Phys. Soc. Jpn.* **84**, 114002 (2015).
44. F. Ofli, R. Chaudhry, G. Kurillo, R. Vidal, R. Bajcsy, Sequence of the most informative joints (SMIJ): A new representation for human skeletal action recognition. *J. Vis. Commun. Image Represent.* **25**, 24–38 (2014).
45. E. Couturier, S. Courrech du Pont, S. Douady, A global regulation inducing the shape of growing folded leaves. *PLOS ONE* **4**, e7968 (2009).
46. K. E. Laflin, C. J. Morris, T. Muqeem, D. H. Gracias, Laser triggered sequential folding of microstructures. *Appl. Phys. Lett.* **101**, 131901 (2012).
47. S. M. Felton, M. T. Tolley, B. Shin, C. D. Onal, E. D. Demaine, D. Rus, R. J. Wood, Self-folding with shape memory composites. *Soft Matter.* **9**, 7688–7694 (2013).
48. K. Yu, A. Ritchie, Y. Mao, M. L. Dunn, H. Jerry Qi, Controlled sequential shape changing components by 3D printing of shape memory polymer multimaterials. *Procedia IUTAM* **12**, 193–203 (2015).
49. T. G. Leong, A. M. Zarafshar, D. H. Gracias, Three-dimensional fabrication at small size scales. *Small* **6**, 792–806 (2010).
50. J. J. Guan, H. Y. He, D. J. Hansford, L. J. Lee, Self-folding of three-dimensional hydrogel microstructures. *J. Phys. Chem. B* **109**, 23134–23137 (2005).
51. L. Ionov, 3D microfabrication using stimuli-responsive self-folding polymer films. *Polymer Rev.* **53**, 92–107 (2013).
52. Y. Liu, J. K. Boyles, J. Genzer, M. D. Dickey, Self-folding of polymer sheets using local light absorption. *Soft Matter.* **8**, 1764–1769 (2012).
53. Y. Lee, H. Lee, T. Hwang, J.-G. Lee, M. Cho, Sequential folding using light-activated polystyrene sheet. *Sci. Rep.* **5**, 16544 (2015).
54. J. J. Champoux, DNA topoisomerases: Structure, function, and mechanism. *Annu. Rev. Biochem.* **70**, 369–413 (2001).
55. Y. Liu, thesis, North Carolina State University, Raleigh, NC (2013).
56. T. Castle, Y. Cho, X. Gong, E. Jung, D. M. Sussman, S. Yang, R. D. Kamien, Making the cut: Lattice *kirigami* rules. *Phys. Rev. Lett.* **113**, 245502 (2014).
57. M. K. Blees, A. W. Barnard, P. A. Rose, S. P. Roberts, K. L. McGill, P. Y. Huang, A. R. Ruyack, J. W. Kevek, B. Kobrin, D. A. Muller, P. L. McEuen, Graphene kirigami. *Nature* **524**, 204–207 (2015).
58. Y. Zhang, Z. Yan, K. Nan, D. Xiao, Y. Liu, H. Luan, H. Fu, X. Wang, Q. Yang, J. Wang, W. Ren, H. Si, F. Liu, L. Yang, H. Li, J. Wang, X. Guo, H. Luo, L. Wang, Y. Huang, J. A. Rogers, A mechanically driven form of Kirigami as a route to 3D mesostructures in micro/nanomembranes. *Proc. Natl. Acad. Sci. U.S.A.* **112**, 11757–11764 (2015).
59. D. Beyer, S. Gurevich, S. Mueller, H.-T. Chen, P. Baudisch, Platener: Low-fidelity fabrication of 3D objects by substituting 3D print with laser-cut plates, in *Proceedings of the 33rd Annual ACM conference on Human Factors in Computing Systems* (ACM, 2015), pp. 1799–1806.
60. L. L. Howell, *Compliant Mechanisms* (Wiley, 2001).
61. A. E. Guérinot, S. P. Magleby, L. L. Howell, R. H. Todd, Compliant joint design principles for high compressive load situations. *J. Mech. Des.* **127**, 774 (2005).
62. Y. Liu, M. Miskiewicz, M. J. Escuti, J. Genzer, M. D. Dickey, Three-dimensional folding of pre-strained polymer sheets via absorption of laser light. *J. Appl. Phys.* **115**, 204911 (2014).
63. D. Davis, B. Chen, M. D. Dickey, J. Genzer, Self-folding of thick polymer sheets using gradients of heat. *J. Mech. Robot.* **8**, 031014 (2016).
64. J. Zhou, S. A. Turner, S. M. Brosnan, Q. Li, J.-M. Y. Carrillo, D. Nykypanchuk, O. Gang, V. S. Ashby, A. V. Dobrynin, S. S. Sheiko, Shapeshifting: Reversible shape memory in semicrystalline elastomers. *Macromolecules* **47**, 1768–1776 (2014).
65. S. A. Turner, J. Zhou, S. S. Sheiko, V. S. Ashby, Switchable micropatterned surface topographies mediated by reversible shape memory. *ACS Appl. Mater. Interfaces* **6**, 8017–8021 (2014).
66. K. K. Westbrook, P. T. Mather, V. Parakh, M. L. Dunn, Q. Ge, B. M. Lee, H. Jerry Qi, Two-way reversible shape memory effects in a free-standing polymer composite. *Smart Mater. Struct.* **20**, 065010 (2011).
67. T. Chung, A. Romo-Uribe, P. T. Mather, Two-way reversible shape memory in a semicrystalline network. *Macromolecules* **41**, 184–192 (2008).
68. H. Meng, G. Li, Reversible switching transitions of stimuli-responsive shape changing polymers. *J. Mater. Chem. A* **1**, 7838–7865 (2013).
69. M. Behl, K. Kratz, J. Zotzmann, U. Nöchel, A. Lendlein, Reversible switching transitions of stimuli-responsive shape changing polymers. *Adv. Mater.* **25**, 4466–4469 (2013).

Acknowledgments: We thank C.-K. Yeung for his help in building the cooling stage for the high-power LEDs. We also thank S. Reece for his help with printer troubleshooting and the Parsons laboratory at North Carolina State University for access to a profilometer. **Funding:** This work was supported by the NSF under the Emerging Frontiers in Research and Innovation program (grant no. 1240438) and by the U.S. Department of Energy (grant no. 08NT0001925). **Author contributions:** Y.L. designed the experiments. Y.L. and B.S. performed the experiments. Y.L. analyzed the data. Y.L., M.D.D., and J.G. wrote the manuscript. M.D.D. and J.G. supervised and oversaw the project. All authors participated in discussions of the research. **Competing interests:** The authors declare that they have no competing interests. **Data and materials availability:** All data needed to evaluate the conclusions in the paper are present in the paper and/or the Supplementary Materials. Additional data related to this paper may be requested from the authors.

Submitted 4 October 2016
Accepted 9 January 2017
Published 3 March 2017
10.1126/sciadv.1602417

Citation: Y. Liu, B. Shaw, M. D. Dickey, J. Genzer, Sequential self-folding of polymer sheets. *Sci. Adv.* **3**, e1602417 (2017).

Sequential self-folding of polymer sheets

Ying Liu, Brandi Shaw, Michael D. Dickey and Jan Genzer

Sci Adv **3** (3), e1602417.
DOI: 10.1126/sciadv.1602417